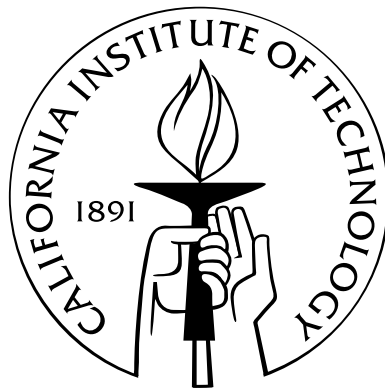


Seasonal Trends in Titan's Atmosphere: Haze, Wind, and Clouds

Thesis by
Antonin Henri Bouchez

In Partial Fulfillment of the Requirements
for the Degree of
Doctor of Philosophy



California Institute of Technology
Pasadena, California

2004
(Defended July 25, 2003)

© 2004

Antonin Henri Bouchez

All Rights Reserved

This dissertation is dedicated to Eleta Trejo-Cantwell, my friend and partner throughout this long and sometimes difficult process.

Abstract

I present an analysis of visible and near-infrared adaptive optics images and spectra of Titan taken over 43 nights between October 1997 and January 2003 with the AEOs 3.6-m, Palomar Hale 5-m, and W.M. Keck 10-m telescopes. These observations reveal a seasonally changing stratospheric haze layer, two distinct regions of condensate clouds in the southern hemisphere, the albedo of Titan's surface, and the zonal wind field of the stratosphere.

Transient convective CH_4 clouds are identified near Titan's south pole, rising to 16 ± 5 km above the surface. These clouds have been continuously present south of 70°S since at least December 2001, currently account for 0.5–1% of Titan's $2 \mu\text{m}$ flux, and appear to be gradually brightening or thickening as the insolation of the south polar region increases. Above the polar clouds, an extensive but optically thin ($\tau \approx 0.05$ at $2 \mu\text{m}$) cloud layer is noted near the tropopause south of 30°S . Aside from the convective CH_4 clouds near the south pole, Titan's troposphere is free of aerosols with an upper limit of $\tau < 0.01$ on the $2 \mu\text{m}$ vertical optical depth in the 5–30 km altitude region.

The albedo of Titan's surface at $2.0 \mu\text{m}$ is derived from the radiative transfer analysis of spatially resolved spectra and images, and presented in the form of a ~ 600 km resolution global surface albedo map. At this resolution, the $2.0 \mu\text{m}$ albedo ranges from 0.05 to 0.17, consistent with extensive exposure of clean water ice in some regions, while hydrocarbons and atmospheric sediments blanket others.

The zonal wind field of Titan's stratosphere near southern summer solstice is derived from adaptive optics observations of the occultation of a binary star on 20 December 2001. Multiple refracted stellar images were detected on Titan's limb during the each successive occultation, allowing the angular deflection of the starlight at two altitudes over both hemispheres to be measured with an uncertainty of ~ 2 milliarcseconds. The zonal wind field derived from this measurement of the shape of Titan's limb exhibits strong but asymmetric high latitude jets, with peak wind speeds of $230 \pm 20 \text{ m s}^{-1}$ at 60°N and $160 \pm 40 \text{ m s}^{-1}$ at

40°S, and lower winds of $110 \pm 40 \text{ m s}^{-1}$ at the equator. The direction of the wind is not constrained.

Acknowledgements

My greatest thanks go to my advisor Mike Brown. For over 10 years, at U.C. Berkeley, the University of Arizona and finally Caltech, Mike has offered me opportunities, challenges, and especially inspiration.

Caitlin Griffith generously allowed me to use and modify her radiative transfer model of Titan's atmosphere, central to much of the analysis presented in this dissertation. Leslie Young provided the initial motivation for the occultation observations, and useful advice on their analysis. Special thanks go to Chad Trujillo, Henry Roe, and Chris Koresko for advice on observational and analytical techniques, and to Mark Richardson and Andy Ingersoll for helpful discussions on atmospheric physics.

Rich Dekany and Mitch Troy built the Palomar adaptive optics system, with which much of the data presented in this dissertation was collected. They frequently participated in the acquisition of the observations, and went out of their way to optimize the hardware for observations of Titan. Without their dedicated efforts, and support of Rick Burruss at Palomar Observatory, little of this work would have been possible.

I am grateful to Chao Bian, Randy Campbell, Joe Carson, Christophe Dumas, Josh Eisner, Bill Forrest, Elise Furlan, Luke Keller, Maciej Konacki, Jean-Luc Margot, David Le Mignant, Stan Metchev, Keven Uchida, and Dan Watson for acquiring images of Titan on their own observing time, providing otherwise unattainable nightly observations of Titan's clouds. I also thank Sarah Hörst, who spent 30 cold winter nights observing Titan from the roof of Robinson Hall, maintaining her enthusiasm throughout.

My six years at Caltech were made much more enjoyable by the companionship of my fellow GPS graduate students, especially Magali Billen, Shane Byrne, Lori Fenton, Elizabeth Johnson, Matt Pritchard, Edwin Shauble, Sarah Stewart-Mukhopadhyay, Anthony Toigo, Ashwin Vasavada, Ben Weiss, and Huiquin Wang. Finally, I thank my friend Ute Zimmermann for inspiration during the final weeks of this effort.

Contents

Abstract	iv
Acknowledgements	vi
1 Introduction	1
1.1 Opening remarks	1
1.2 Methods	3
1.2.1 Adaptive optics	3
1.2.2 Radiative transfer calculations	4
2 Visible adaptive optics observations of Titan’s atmosphere and surface	5
2.1 Introduction	5
2.2 Observations and data reduction	7
2.2.1 AEOS adaptive optics system	7
2.2.2 Data reduction	9
2.2.3 Filters	12
2.3 Results	13
2.3.1 Stratosphere	13
2.3.2 Troposphere	15
2.3.3 Surface	18
2.4 Conclusions	24
3 Spatially resolved spectroscopy of Titan	27
3.1 Introduction	27
3.2 Observations	29
3.3 Data reduction	31

3.3.1	Images	31
3.3.2	Spectra	33
3.4	Analysis	36
3.4.1	Spectral diversity	36
3.4.2	Radiative transfer	39
3.4.3	PSF estimation	39
3.4.4	Model optimization	40
3.5	Results	41
3.5.1	Mean atmosphere	41
3.5.2	Zonal haze model	43
3.5.3	Surface albedo	45
3.6	Discussion	48
3.6.1	Seasonal change in Titan's haze	48
3.6.2	Tropopause cirrus	49
3.6.3	Surface	50
3.7	Conclusions	51
4	Titan's stratospheric winds	52
4.1	Introduction	52
4.1.1	Stellar occultations	52
4.1.2	Region of atmosphere probed	55
4.1.3	3 July 1989 Titan occultation	56
4.1.4	20 December 2001 Titan occultation	56
4.2	Observations	58
4.2.1	Adaptive optics	58
4.2.2	Timing	59
4.3	Data reduction	60
4.3.1	Bias and gain correction	60
4.3.2	Titan disk model	61
4.3.3	PSF determination	61
4.3.4	Relative position and flux of stars	62
4.4	Model	64

4.4.1	General approach	64
4.4.2	Coordinate systems	67
4.4.3	Deflection angle and flux	69
4.4.4	Atmospheric model	70
4.4.5	Wind model	72
4.4.6	Numerical solution	74
4.4.7	Geometric and instrumental effects	76
4.4.8	Model fitting	79
4.5	Results	81
4.5.1	Uniformly rotating atmosphere	81
4.5.2	Non-uniform wind model	84
4.5.3	Stellar properties	87
4.6	Discussion	88
4.7	Conclusions	90
5	Direct detection of variable tropospheric clouds near Titan's south pole	92
5.1	Introduction	92
5.2	Observations	93
5.3	Results	93
5.4	Discussion	96
5.5	Acknowledgements	99
6	Seasonal changes in Titan's tropospheric clouds	100
6.1	Introduction	100
6.2	Observations	101
6.2.1	Palomar adaptive optics images, 2001–2003	101
6.2.2	Keck speckle images, 1997–1998	104
6.2.3	Keck adaptive optics images, 2002	105
6.3	Analysis	105
6.3.1	Surface albedo map	105
6.3.2	Titan's lightcurve	109
6.3.3	PSF determination	110
6.3.4	Cloud positions and fluxes	114

6.4	Discussion	114
6.4.1	Cloud location	114
6.4.2	Cloud size	115
6.4.3	Seasonal evolution	117
6.4.4	Tropospheric wind	118
6.5	Conclusions	119
7	A photometric search for clouds on Titan	121
7.1	Introduction	121
7.2	Observations	123
7.3	Data reduction	127
7.4	Analysis	131
7.5	Conclusions	134
A	Thesis data	136
A.1	Spatially resolved spectra	136
A.2	20 December 2001 occultation	136
A.3	Adaptive optics and speckle images at $2 \mu\text{m}$	137
	Bibliography	138

List of Figures

1.1	Rapid advances in high resolution imaging	1
2.1	AEOS nightly mean images of Titan	11
2.2	AEOS filters	12
2.3	Opacity of Titan’s atmosphere in AEOS filters	14
2.4	Stratospheric haze 2000–2001	15
2.5	AEOS images of tropospheric scattering	17
2.6	AEOS images of Titan’s surface	19
2.7	Effective phase function of surface images	21
2.8	Map of relative 940 nm surface albedo	22
2.9	Relative 940 nm surface albedo uncertainty	22
2.10	Photometry of four representative locations	23
3.1	Palomar AO broad-band images of Titan	32
3.2	Comparison of resolved spectra of Titan’s limb	37
3.3	Narrow-band images of Titan from spectra	38
3.4	Mean haze profiles	42
3.5	Optical depth of haze versus latitude	43
3.6	Sample haze profiles	44
3.7	Altitude of tropospheric scattering layer	45
3.8	Surface albedo distribution	46
3.9	Sample model fits to spectra	47
4.1	Titan occulting a binary star	53
4.2	Region of Titan’s atmosphere probed by stellar occultation	55
4.3	Limb shape and zonal winds from the 28 Sgr occultation	57

4.4	Tracks of Titan's shadows	58
4.5	Deconvolved model of Titan's disk	61
4.6	Titan-subtracted occultation image sequence	63
4.7	Relative position and flux of stars	65
4.8	Temperature of Titan's lower stratosphere	67
4.9	Path-integrated refractivity through a Titan-like atmosphere	75
4.10	Predicted flux in the observer plane	76
4.11	Predicted positions and flux, uniformly rotating atmosphere	83
4.12	Residuals in detector coordinates, uniform wind	83
4.13	Uniform wind model	84
4.14	Residuals in planet plane, uniform wind	85
4.15	Predicted positions and flux, non-uniform wind	86
4.16	Residuals in detector coordinates, non-uniform wind	86
4.17	Non-uniform wind model	88
5.1	Keck AO images of transient clouds on Titan	94
5.2	Polar projections of cloud images	95
5.3	Spectrum of Titan's south polar clouds	97
6.1	Palomar AO images of Titan 2002–2003	103
6.2	Keck speckle images of Titan 1997–1998	104
6.3	Keck AO images of Titan in 2002	105
6.4	Low-resolution map of Titan's 2.0 μm surface albedo	108
6.5	High resolution map of Titan's 2.0 μm surface albedo	108
6.6	Titan's rotational lightcurve	109
6.7	Palomar image models and PSFs. I.	111
6.8	Palomar image models and PSFs. II.	112
6.9	Keck speckle image models and PSFs	113
6.10	Keck AO image models and PSFs	114
6.11	Polar stereographic projection of cloud locations	115
6.12	Average daily insolation on Titan	118
6.13	Images of Titan separated by one rotation	119

7.1	Sample C-14 images of Titan	122
7.2	C-14 filters	123
7.3	C-14 image processing	127
7.4	Sample raw C-14 photometry	128
7.5	Sample C-14 flux ratios	129
7.6	Titan's raw 795 nm flux over 81 nights	130
7.7	Correlation between extinction and Titan's apparent color	131
7.8	Corrected nightly-mean flux ratio of Titan	132
7.9	Flux ratios, with respect to orbital phase	133
7.10	Flux ratios, with surface lightcurve subtracted	133

List of Tables

2.1	AEOS observations	8
2.2	AEOS Filters	12
3.1	Palomar AO spectroscopic observations	30
3.2	Radiative transfer model parameters	41
4.1	Variables used in the occultation model	67
4.2	Free and fixed occultation model parameters	80
4.3	Uniform wind model	81
4.4	Non-uniform wind model	87
6.1	Palomar AO observations	102
6.2	Keck speckle observations	102
6.3	Keck AO observations	102
6.4	Position and flux of detected transient clouds	116
7.1	C-14 observations. I.	124
7.1	C-14 observations. II.	125
7.1	C-14 observations. III.	126